

See discussions, stats, and author profiles for this publication at: <https://www.researchgate.net/publication/10650342>

# Calibration and Evaluation of Nitric Acid and Ammonia Permeation Tubes by UV Optical Absorption

ARTICLE *in* ENVIRONMENTAL SCIENCE AND TECHNOLOGY · JULY 2003

Impact Factor: 5.33 · DOI: 10.1021/es026422l · Source: PubMed

---

CITATIONS

27

---

READS

50

7 AUTHORS, INCLUDING:



[Jonathan Andrew Neuman](#)

National Oceanic and Atmospheric Administr...

126 PUBLICATIONS 3,105 CITATIONS

SEE PROFILE



[John B. Nowak](#)

Aerodyne Research, Inc.

103 PUBLICATIONS 2,029 CITATIONS

SEE PROFILE



[Fred C. Fehsenfeld](#)

503 PUBLICATIONS 25,100 CITATIONS

SEE PROFILE

# Calibration and Evaluation of Nitric Acid and Ammonia Permeation Tubes by UV Optical Absorption

J. ANDREW NEUMAN,<sup>\*,†,‡</sup>THOMAS B. RYERSON,<sup>†</sup>L. GREGORY HUEY,<sup>§</sup> ROGER JAKOUBEK,<sup>†</sup>JOHN B. NOWAK,<sup>†</sup> CRAIG SIMONS,<sup>†,‡</sup> ANDFREDERICK C. FEHSENFELD<sup>†,‡</sup>

NOAA Aeronomy Laboratory, Boulder, Colorado 80305,  
CIRES, University of Colorado, Boulder, Colorado 80309, and  
School of Earth and Atmospheric Sciences, Georgia Institute of  
Technology, Atlanta, Georgia 30332

An ultraviolet (UV) optical absorption system has been developed for absolute calibrations of nitric acid ( $\text{HNO}_3$ ) and ammonia ( $\text{NH}_3$ ) permeation tube emission rates. Using this technique, dilute mixtures containing  $\text{NH}_3$  or  $\text{HNO}_3$ , both of which interact strongly with many surfaces, are accurately measured at levels below a part per million by volume. This compact and portable instrument operates continuously and autonomously to rapidly ( $<1$  h) quantify the emission of trace gases from permeation devices that are commonly used to calibrate air-monitoring instruments. The output from several  $\text{HNO}_3$  and  $\text{NH}_3$  permeation tubes, with emission rates that ranged between 13 and 150 ng/min, was examined as a function of temperature, pressure, and carrier gas flow. Absorptions of 0.015% can be detected which allows a precision ( $3\sigma$ ) of  $\pm 1$  ng/min for the  $\text{HNO}_3$  and  $\text{NH}_3$  permeation tubes studied here. The accuracy of the measurements, which relies on published UV absorption cross sections, is estimated to be  $\pm 10\%$ . Measurements of permeation tube emission rates using ion chromatography analysis are made to further assess measurement accuracy. The output from the  $\text{HNO}_3$  and  $\text{NH}_3$  permeation tubes examined here was stable over the study period, which ranged between 3 months and 1 year for each permeation tube.

## Introduction

Accurate measurements of trace gases in the atmosphere are achieved by quantifying the detection sensitivity of air-sampling instruments. Repeated standard addition calibrations of instruments, performed at mixing ratios relevant to atmospheric conditions and under a variety of ambient conditions, ensure measurement accuracy and yield information on the dependence of the instrument's sensitivity to different ambient matrices. Permeation devices, which deliver pure gases at a fixed rate through a permeable membrane, are particularly useful for generating gas standards at low mixing ratios typical of the atmosphere. Using permeation devices for instrument calibration offers several advantages

over using gas standards contained in cylinders. In gas cylinders, the trace components in low-level mixtures may adsorb onto the cylinder walls and compromise calibration accuracy. Furthermore, because permeation devices are small compared to gas cylinders, they are useful for instruments that must be compact and lightweight. For example, calibration systems using permeation devices have been built into portable ground-based and aircraft-based instruments (1–3) that perform in-situ measurements of atmospheric trace gases. For a permeation tube to be valuable for generating gas standards for instrument calibration purposes, the emission rate from the permeation tube must be known.

The calibration of permeation tube emission rates can be challenging, since the emission rates must often be quite low in order to provide trace gases at levels comparable to their atmospheric abundance. For example, nitric acid ( $\text{HNO}_3$ ) and ammonia ( $\text{NH}_3$ ) permeation tubes that emit 23 ng/min and 6 ng/min, respectively, provide a 1 part per billion by volume (ppbv) mixing ratio (characteristic of many urban environments) when diluted into an 8 standard liter per minute (slpm) flow. Consequently, a calibration system must be able to measure permeation rates that range from a few ng/min to tens of ng/min. An air-monitoring instrument requires even greater sensitivity and selectivity than the calibration system reported here, as it must be capable of measuring the calibration gas diluted to the ppbv or parts per trillion by volume (pptv) level in an ambient air mixture.

Several techniques have been employed to quantify the emission rate of trace gases from permeation devices. By measuring the change in weight of a permeation tube as a function of time, gravimetric methods have been used to determine permeation tube emission rates (4, 5). However, if the gas in the permeation device is not pure, contamination gases such as  $\text{H}_2\text{O}$  or  $\text{CO}_2$  that also permeate through the membrane will cause calibration errors (6). Additionally, permeation tubes with low emission rates (tens of ng/min) may require weighing over long periods to obtain measurable weight loss. Ion chromatography (IC) has been employed for the purpose of determining permeation tube emission rates (1–3). For water-soluble species, the output of a permeation tube can be bubbled through water and analyzed by IC. However, the hours required to collect a sufficiently large sample for analysis (1) and the required instrumentation and analysis time makes this technique inconvenient for continuous monitoring to assess permeation tube stability.

Permeation tube emission rates are determined here using a compact and portable instrument that relies on the optical absorption of ultraviolet (UV) light. This technique is applicable to gases that absorb light in the UV with a known absorption cross section. The instrument described here is derived from photometers that are commonly used to determine ozone mixing ratios in the atmosphere (7) and gas number densities in laboratory experiments (8, 9). This system allows for continuous monitoring of permeation tube output so that potential changes in permeation rate, which have been observed in some permeation devices (5, 6), can be immediately detected and quantified. By using an absolute measurement to examine permeation tube output, instrument calibrations are based on published absorption cross sections, rather than on calibration gases contained in gas cylinders that are subject to deterioration or depletion over time. Furthermore, this system measures the gas concentration that is delivered to an instrument and thus tests the entire calibration system including all the gas handling components. The Teflon flow system and absorption cell allows for rapid measurements of the number density of

\* Corresponding author phone: (303)497-7872; fax: (303)497-5126; e-mail: neuman@al.noaa.gov.

<sup>†</sup> NOAA Aeronomy Laboratory.

<sup>‡</sup> CIRES.

<sup>§</sup> Georgia Institute of Technology.

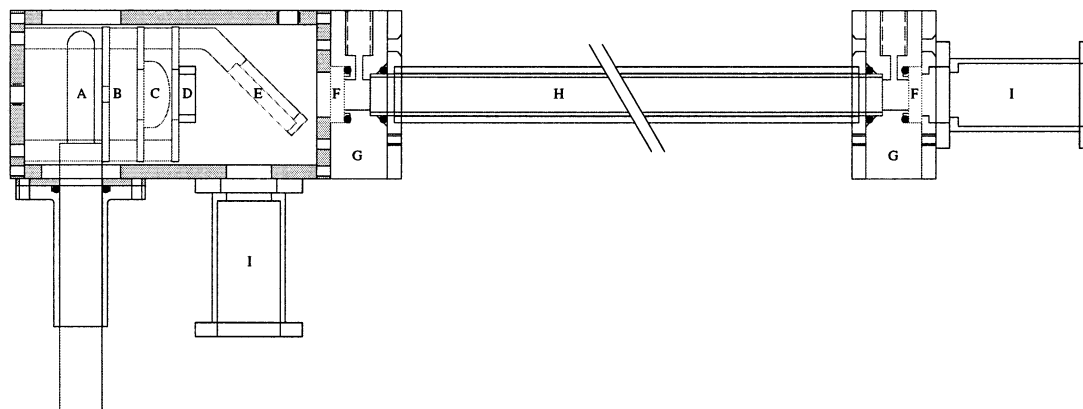


FIGURE 1. UV absorption cell. Light from a Hg lamp (A) and aperture (B) is collimated by plano-convex lens (C). A 185 nm interference filter (D) transmits only the 185 nm line from the lamp. A beam splitter (E) permits the lamp intensity to be monitored by the reference detector. The absorption cell (H) is sealed by Teflon O-rings and fused silica windows (F) held in Teflon mounts (G). The phototubes (I) detect both the transmitted and reflected light that is incident on the beam splitter.

parts per million by volume (ppmv) levels of gases that readily react with surfaces ( $\text{HNO}_3$  or  $\text{NH}_3$ ).

### Principle of Operation

Permeation tube emission rates are measured by constantly flowing nitrogen ( $\text{N}_2$ ) over a thermostated permeation tube and through an optical absorption cell. The number density of light-absorbing molecules in the cell ( $n$ ) is determined from Beer's Law

$$\frac{I}{I_0} = e^{-\sigma nL} \quad (1)$$

where  $I$  is the intensity of light transmitted through the absorption cell in the presence of the absorbing gas,  $I_0$  is the intensity of light in the absence of the absorber,  $\sigma$  is the absorption cross section for the absorber in the cell, and  $L$  is the length of the cell. In this work,  $I$ ,  $I_0$ , and  $L$  are measured, and  $\sigma$  is taken from published data in order to determine  $n$ . The  $\sigma$  used here is for the line center of the spectrally narrow (compared to broad molecular absorption features) atomic lamp emission. Using the Ideal Gas Law and the dilution of the permeation tube emission by the  $\text{N}_2$  carrier gas flow, the number density of molecules in the absorption cell resulting from permeation tube emission also can be written as

$$n = 2.16 \times 10^{14} \times \frac{pE}{TFM} \quad (2)$$

In eq 2, the emission rate  $E$  is in ng/min, the carrier gas flow  $F$  is in standard  $\text{cm}^3/\text{min}$  (sccm), the molecular weight of the absorbing molecules ( $M$ ) is in g/mol, the pressure ( $p$ ) is in Torr, and the temperature ( $T$ ) of the gas in the absorption cell is in K. Combining Beer's Law (eq 1) and the Ideal Gas Law, the emission is written in terms of  $\sigma$  ( $\text{cm}^2$ ) and  $L$  (cm) as

$$E = -4.62 \times 10^{-15} \times \ln\left(\frac{I}{I_0}\right) \times \frac{TFM}{p\sigma L} \quad (3)$$

By measuring the absorption of the 184.95 nm atomic line from a low-pressure mercury (Hg) lamp, emission rates for  $\text{HNO}_3$  and  $\text{NH}_3$  permeation tubes are determined, using reported absorption cross sections at 185 nm. The absorption cross section for  $\text{HNO}_3$  has been measured by Biaueme (10) to be  $1.63 \times 10^{-17} \text{ cm}^2$  with an experimental uncertainty of  $\pm 3\%$ . Subsequent measurements by Burkholder et al. (11) and Wine et al. (9) have confirmed this value. The  $\text{NH}_3$  cross section was measured by Lovejoy (12) to be  $4.2 \times 10^{-18} \text{ cm}^2$

and by Froyd (13) to be  $4.67 \times 10^{-18} \text{ cm}^2$ , both of which are in agreement with previous measurements by Tannenbaum et al. (14). An average value of  $4.4 \pm 0.3 \times 10^{-18} \text{ cm}^2$  is used for the 185 nm  $\text{NH}_3$  cross section here.

### Experimental Section

Since many molecules have large absorption cross sections in the UV,  $I/I_0$  is measured using the 184.95 nm atomic line from a low-pressure mercury (Hg) discharge lamp. While these discharge lamps can be obtained in small packages (approximately 8 cm long, 1 cm diameter), light emerges from a large volume (approximately 2.5 cm long, 0.6 cm diameter) that makes imaging the source difficult. Consequently, a 0.3 cm diameter aperture is placed approximately 5 cm from the lamp to reduce the angle from which the light emerges. A quartz lens with a 20 cm focal length collimates the light that passes through the aperture, and a 185 nm band-pass interference filter is placed after the collimating lens to attenuate other Hg atomic lines emitted by the lamp. A quartz window is used as a beam splitter to reflect some of the lamp light to a reference detector that monitors the Hg lamp intensity. The lamp housing is continuously flushed with a 20 sccm flow of  $\text{N}_2$  to prevent absorption of the 185 nm light by oxygen ( $\text{O}_2$ ) or the formation of ozone from  $\text{O}_2$  photolysis at 185 nm. The lamp housing is also temperature-controlled to reduce changes in lamp intensity that occur with changes in lamp temperature. The light transmitted through the beam splitter goes through the absorption cell and on to a detector at the cell exit, as shown in Figure 1.

Since absorption cross sections vary with wavelength, it is important to be certain of the spectral characteristics of the detected light. The detectors, which are phototubes with a cesium-iodide photocathode and a quartz window, have a spectral response from 160 to 200 nm, with a peak at 165 nm. These phototubes are sensitive to the 185 nm Hg line and discriminate against other wavelengths emitted by the lamp. The interference filter at the entrance to the cell further guarantees that only the 185 nm line is measured. The interference filters typically have a bandwidth of 20 nm full width at half-maximum, a peak transmission of 15% at 185 nm, and a transmission of 0.015% at 254 nm, where a strong Hg line exists.

The absorption cell used here is made from thin wall perfluoro-alkoxy Teflon (PFA) tube (i.d. = 0.79, o.d. = 0.95 cm) to allow for use with  $\text{HNO}_3$  and other gases that may interact on the surfaces of many materials. The PFA tube is held in an aluminum sleeve that can be temperature controlled. For the results shown here, the absorption cell was at 34 °C. The cell length is 25.4 cm. The cell windows,

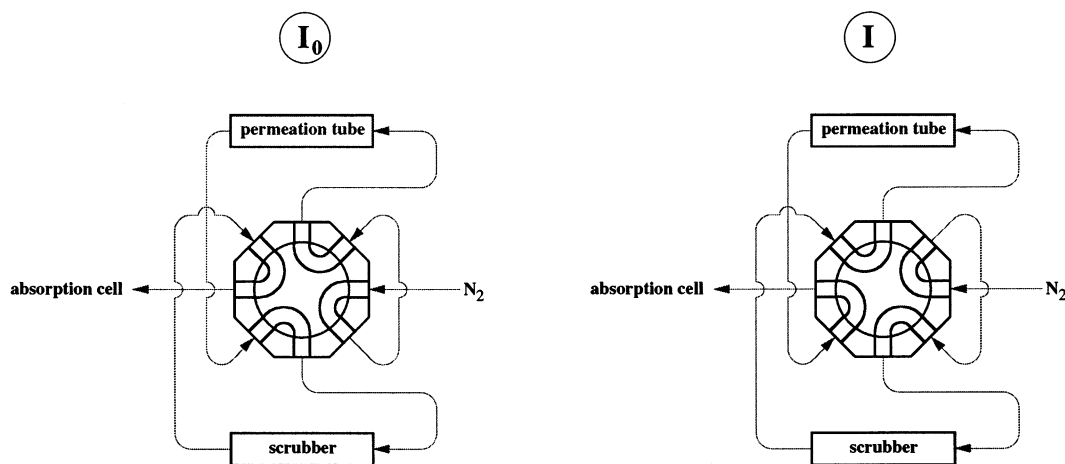


FIGURE 2. 8-port valve schematic for admitting gas into the absorption cell. All wetted surfaces are Teflon. During measurements of  $I_0$ , the valve directs the  $N_2$  carrier gas first through the permeation tube followed by the scrubber and then into the absorption cell. During measurements of  $I$ , the  $N_2$  carrier gas is first sent through the scrubber so that the output from the permeation tube flows through the absorption cell.

which are made from fused silica, are pressed against Teflon O-rings in Teflon mounts that contain fittings for the 0.32 cm o.d. PFA tubes that deliver gas to and from the absorption cell.

The number density of absorbers in the cell is determined using the ratio of the transmitted light in the presence and absence of the absorbers. In all cases, dry  $N_2$  is used as the carrier gas that sweeps over the permeation tube and into the absorption cell. If the permeation tube emits no absorbers other than the gas to be measured, then  $I_0$  can be determined by flushing the absorption cell with  $N_2$ . However, if the permeation tube emits other gases (for example  $H_2O$ ,  $NO_2$ , or  $O_2$ ) that absorb at 185 nm, then  $I_0$  must be determined by selectively scrubbing the absorber to be measured. A computer controlled Teflon 8-port valve at the cell entrance is used to switch gas flows and accommodates either flushing with  $N_2$  or scrubbing the absorber for determining  $I_0$ . Figure 2 illustrates the valve positions for measuring  $I$  and  $I_0$  using a scrubber to remove the permeation tube output from the gas stream. The  $N_2$  gas always flows in the same direction through the permeation tube oven, scrubber, and absorption cell, and activating the valve only changes the order of the flow through the permeation tube and scrubber. This use of the scrubber to determine  $I_0$  makes the system insensitive to the presence of impurities or the release of surface-adsorbed gases from any of the components of the calibration system upstream of the scrubber.

Signals from the phototubes are amplified, converted to voltages, and computer recorded at 5 s intervals. The amplifiers include an RC integrator with a 5 s time constant that averages much of the rapid fluctuations in the lamp output. The computer also records the pressure in the absorption cell and the output voltage from the mass flow controller that determines the  $N_2$  flow through the permeation tube and absorption cell.

The permeation tubes used here are commercially available steel and Teflon tubes that hold liquid  $HNO_3$  or  $NH_3$  (Kin-Tek, LaMarque, Texas). Six  $HNO_3$  and three  $NH_3$  permeation tubes were examined extensively under many different flows, pressures, and temperatures. The tubes were never heated greater than 50 °C, as recommended by the manufacturer. When not in use, the permeation tubes were stored individually in sealed containers at room temperature. During use, the permeation tubes were placed in a temperature controlled oven with all wetted materials made from Teflon. The ovens are made from a 0.84 cm i.d. Teflon sleeve pressed into an aluminum block that is temperature con-

trolled to  $\pm 0.1$  °C. The oven is connected to the 8-port valve (Figure 2) through Teflon fittings and 10-cm long sections of 0.32 cm o.d., 0.16 cm i.d. Teflon tubing. The valve, delivery lines, and scrubber were operated at room temperature (20–24 °C), which was sufficient to prevent condensation of these gases on Teflon surfaces (15).

The  $HNO_3$  permeation tubes are made from fluorinated ethylene propylene Teflon (FEP) tubing with 2.5 cm long stainless steel crimps at the ends. In the higher emission rate tubes ( $> 50$  ng/min at 40 °C),  $HNO_3$  permeates through 2–5 cm lengths of 0.47 cm o.d. FEP tube. In the tubes with lower emission rates ( $< 50$  ng/min at 40 °C),  $HNO_3$  permeates through 2 cm lengths of 0.64 cm o.d. FEP tube. The total length of the permeation tubes varies between 6 and 10 cm. The  $HNO_3$  permeation tubes also contain sulfuric acid to sequester water that may be present with the liquid  $HNO_3$ . The  $NH_3$  permeation tubes are made from 8 cm long tubes with Teflon end caps. A stainless steel crimp with a 0.74 cm o.d. surrounds the entire length of the tube, and  $NH_3$  permeates only through the Teflon end caps. The  $NH_3$  permeation tubes are filled with anhydrous  $NH_3$ .

The optical absorbers are removed from the gas stream that flows through the absorption cell by diverting the permeation tube output contained in the  $N_2$  carrier gas through a scrubber. The scrubbers are made from 10 cm long, 0.4 cm i.d. nylon tubes filled with material that selectively absorbs the gas emitted by the permeation tube. The  $HNO_3$  scrubbing material is nylon wool soaked in a saturated aqueous solution of sodium bicarbonate and subsequently dried with a flow of  $N_2$ . These scrubbers have been exposed to a 1 ppmv concentration of  $HNO_3$ , typical of these measurements, for at least several weeks and for as long as several months before becoming saturated with  $HNO_3$ . Consequently, the  $HNO_3$  scrubbers are replaced monthly.

The  $NH_3$  scrubbing material is obtained from silicon phosphates that release phosphoric acid when exposed to humidity (Perma Pure Incorporated, Toms River, NJ). The humidity in the  $N_2$  was sufficient to produce enough phosphoric acid to completely remove  $NH_3$  from the gas stream. Citric acid was also used to scrub  $NH_3$ , but citric acid saturated more rapidly than phosphoric acid. Citric acid scrubbers could completely remove mixing ratios of approximately 1 ppmv of  $NH_3$  for only a few days before failing, whereas the phosphoric acid scrubbers were effective for many months.

The effectiveness of these  $HNO_3$  and  $NH_3$  scrubbers were tested in several ways. Signals obtained with only  $N_2$  flowing



through the absorption cell were equivalent to signals obtained with  $\text{N}_2$  flowing through the permeation tube and scrubber before entering the absorption cell. This demonstrated that the output from the permeation tube was completely removed by the scrubber. The scrubber effectiveness was also demonstrated by varying the amount of  $\text{HNO}_3$  and  $\text{NH}_3$  sent through the scrubber without causing a change in either  $I$  or  $I_0$ . When the scrubber was downstream of the permeation tube, the absorption cell signal was unchanged when the permeation tube temperature was elevated to increase the output by over a factor of 2.

Accurate measurements are achieved only if the difference between  $I$  and  $I_0$  are solely due to the 184.95 nm atomic Hg line transmitted through the cell. Potential interferences include detector dark current, detection of other Hg lines, and the loss of the absorber on surfaces within the cell. Detector dark current is measured here both by switching the lamp off and by placing a shutter in front of the lamp. Detector dark current is subtracted from the detector signals and is less than 0.2% of the total signal. Care must be taken to be certain that the 254 nm Hg line, which is approximately 15 times more intense than the 184.95 nm line (BHK, Inc., Claremont, CA), is not detected. The absorption cross section for  $\text{HNO}_3$  and  $\text{NH}_3$  decrease several orders of magnitude from 185 to 254 nm (10, 11) so that detected 254 nm light would reduce the measured absorption and result in a derived permeation rate that is spuriously low. Measurements have been performed with additional 185 nm interference filters placed at the detectors. These filters that transmit 15% at 185 nm reduce the signal intensity by 85%, indicating that the detector signals are entirely from the 185 nm line from the Hg lamp. Additionally, the measured absorptions are unchanged when additional interference filters were placed at the detectors, further confirming that only 185 nm light was detected. The combination of solar-blind phototubes with one 185 nm interference filter eliminates interferences from the 254 nm Hg line.

The imprecision in the differential measurement,  $I/I_0$ , limits the minimum detectable concentration of a trace gas in the absorption cell.  $I$  and  $I_0$  are determined by normalizing the signal from the cell detector by the signal from the reference detector that monitors the lamp intensity. This eliminates changes in signal caused by lamp fluctuations so that  $I$  and  $I_0$  are measured precisely to enable detection of small absorptions. The lower limit of detection for absorption is approximately 0.015%, as calculated from 3 times the standard deviation of the ratio of the cell signal to the reference detector signal measured during a 10-min period. Drifts in signals that occur on time scales longer than the cycling between  $I$  and  $I_0$  do not affect the differential measurement or the instrument performance. For typical cell pressures (835 hPa), temperatures (300 K), and flows (20–50 sccm), this imprecision on the absorption yields a minimum detectable emission of approximately  $\pm 1$  ng/min (3 $\sigma$ ) for both  $\text{HNO}_3$  and  $\text{NH}_3$  permeation tubes.

## Results

An example of the data that were acquired to calibrate permeation tubes is shown in Figure 3. Data were recorded once every 5 s. Figure 3a shows the signals on the cell and reference detectors recorded over 16 h during the calibration of a  $\text{NH}_3$  permeation tube. The high-frequency fluctuations in the absorption cell signal are caused by fluctuations in the lamp intensity, which are also seen in the reference signal in Figure 3a. These rapid lamp-intensity fluctuations do not appear in the ratio of the cell signal to the reference signal, shown in Figure 3b. The valve was actuated every 20 min to alternate between measurements of  $I$  and  $I_0$ , so that the permeation tube emission rate was determined once every 40 min. The values for  $I$  and  $I_0$  used to determine the emission

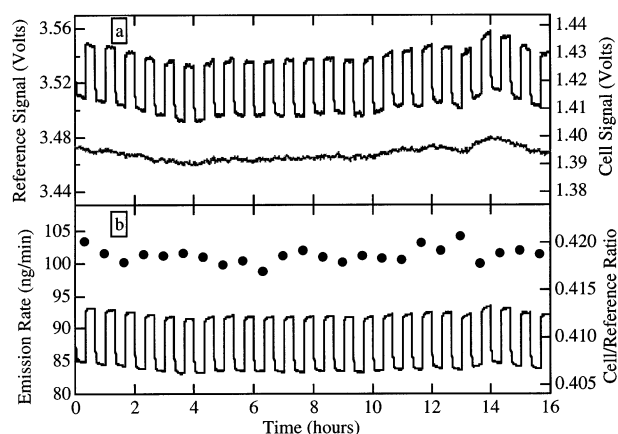


**FIGURE 3.** Reference and cell detector signals (a) versus time. The cell signal is a black line and plotted on the right axis, and the reference signal is a gray line plotted on the left axis. Panel b shows the derived emission rate from this  $\text{NH}_3$  permeation tube on the left axis and the ratio of the cell signal to the reference signal on the right axis. The valve was actuated every 20 min to switch the  $\text{NH}_3$  in and out of the absorption cell.

rate (eq 3) were obtained by averaging the ratio of the cell signal to reference signal for the last 100 s of each 20 min period. A linear interpolation between successive measurements of  $I_0$  was performed to determine the value of  $I_0$  corresponding to each measurement of  $I$ . During measurements of  $I_0$ , the cell signal was elevated when the scrubber removed the  $\text{NH}_3$  from the gas stream. During measurements of  $I$ , the scrubber was upstream of the permeation tube (Figure 2), and  $\text{NH}_3$  was admitted into the cell. Consequently, the signal dropped when  $\text{NH}_3$  absorbed a small ( $\sim 1.4\%$ ) fraction of the light. The derived emission rate for this permeation tube was  $102 \pm 1$  ng/min, as shown in Figure 3b. The  $\text{N}_2$  carrier gas flow was 20 sccm, such that the  $\text{NH}_3$  mixing ratio in the cell was approximately 7 ppmv.

When the six  $\text{HNO}_3$  and three  $\text{NH}_3$  permeation tubes were held at a constant temperature, no changes in their output were observed during the periods in which they were monitored. The  $\text{NH}_3$  permeation tubes were studied for a 3-month period, and each  $\text{HNO}_3$  permeation tube was studied for at least 3 months and up to 1 year. Both the absorption cell and the permeation tubes were occasionally subjected to deliberate interruptions of gas flow, changes in pressure, and changes in temperature. Even when permeation tubes were removed from their ovens and placed in storage for periods ranging from days to months, their output always returned to the same value when they were reinstalled in the ovens. Although the stability of permeation tubes for periods greater than 1 year has not been carefully evaluated here, it is evident that the output from these devices eventually changes. When  $\text{HNO}_3$  permeation tubes were measured before and after being placed in storage for 2 years, their emission rate decreased approximately 30%.

Gases were admitted and removed from the absorption cell with a 20 min period to allow the condensable gases to completely passivate the surfaces. For a 20 sccm flow and a cell pressure of 835 hPa, the flush time of the  $12 \text{ cm}^3$  absorption cell is approximately 30 s. Figure 4 shows the time response of the system for measurements with  $\text{N}_2\text{O}$  and  $\text{HNO}_3$ . Whereas the system equilibrates to the presence or absence of  $\text{N}_2\text{O}$  (which is unreactive on surfaces) within 2 min, approximately 10 min are required for the system to equilibrate to a change in  $\text{HNO}_3$  concentration in the cell. For this reason, the valve is actuated every 15 or 20 min to guarantee that the surfaces are completely passivated so that absorption measurements are determined when the system is in steady-state.

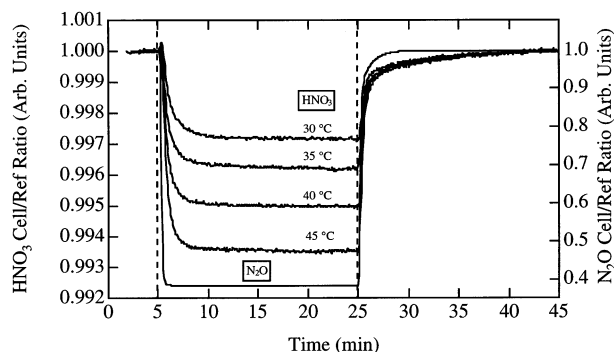


FIGURE 4. The normalized ratio of the cell detector signal to the reference detector signal (cell/ref ratio) versus time. The absorption caused by a dilute mixture of  $\text{N}_2\text{O}$  in  $\text{N}_2$  is plotted on the right axis to illustrate the flush time of the system. The absorption caused by the output from an  $\text{HNO}_3$  permeation tube controlled at four different temperatures is plotted against the left axis. When the  $\text{HNO}_3$  permeation tube temperature was increased from 30 °C to 45 °C, the absorption increased from approximately 0.25% to 0.65%.

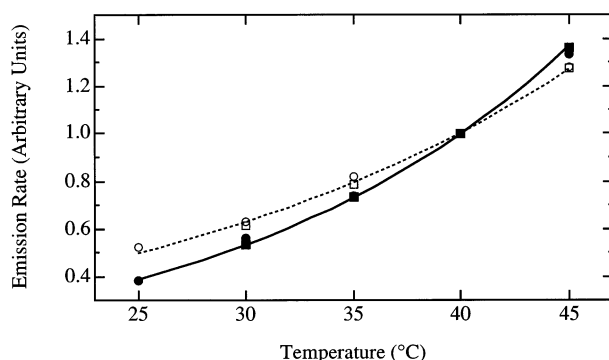


FIGURE 5. Relative emission rates from  $\text{NH}_3$  permeation tubes (open symbols) and  $\text{HNO}_3$  permeation tubes (closed symbols) as a function of permeation tube temperature. The dashed line is a linear least-squares fit to the logarithm of the  $\text{NH}_3$  data, and the solid line is a fit to the  $\text{HNO}_3$  data.

The temperature dependence of permeation tube emission rates has been evaluated. The output from permeation tubes depends both on the vapor pressure of the gas inside the permeation tube and the permeability of the membrane. Since both the vapor pressure of a gas over a liquid and the permeability of Teflon increase roughly exponentially with temperature, permeation tube output is strongly temperature dependent. An example of the measured signals during tests of the temperature dependence of  $\text{HNO}_3$  emission from a permeation tube is shown in Figure 4. At 5 min, the 8-port valve was actuated so that the scrubber was upstream of the permeation tube, and  $\text{HNO}_3$  molecules were admitted into the cell for a measurement of  $I$ . Well after the  $\text{HNO}_3$  equilibrated in the cell, the valve was switched again at 25 min, whereupon the scrubber removed the  $\text{HNO}_3$  from the permeation tube, and  $I_0$  was determined. The  $\text{HNO}_3$  emission increased from approximately 19 ng/min at 30 °C to 43 ng/min at 45 °C. The  $\text{N}_2$  carrier gas flow was 20 sccm, so that the mixing ratio of  $\text{HNO}_3$  in the cell varied from 0.3 to 0.8 ppmv for the measurements shown in Figure 4. The emission rates from the permeation tubes studied here stabilized almost immediately (<20 min) following a moderate ( $\leq 10$  °C) change in temperature.

Figure 5 shows measurements of permeation tube emission rates as a function of temperature for several  $\text{HNO}_3$  and  $\text{NH}_3$  permeation tubes. The open symbols are  $\text{NH}_3$  emission rates and the closed symbols are  $\text{HNO}_3$  emission rates, where all the rates have been normalized to 1 at 40 °C. The lines are linear least-squares fits to the logarithm of the data. The

$\text{HNO}_3$  emission rates are fit by an exponential that doubles every 12 °C, and the  $\text{NH}_3$  emission rates are fit by an exponential that doubles every 14 °C. The trend in these results is consistent with the known vapor pressure curves for  $\text{HNO}_3$  and  $\text{NH}_3$  (16).  $\text{HNO}_3$  vapor pressure doubles every 14.7 °C between 30 °C and 50 °C, and  $\text{NH}_3$  vapor pressure doubles every 23.9 °C between 30 °C and 50 °C. As expected, emission from the permeation tubes increased with temperature more rapidly than the increase in vapor pressure, since Teflon permeability also increases with temperature.  $\text{HNO}_3$  emission rates increased more rapidly with temperature than did  $\text{NH}_3$  emission rates, which is consistent with the difference in vapor pressure for these two compounds.

## Discussion

The accuracy of these measurements is dependent upon the accuracy of the reported absorption cross section and the measured flows, pressures, temperatures, and cell length. The sum of the experimental errors associated with determining flow, pressure, temperature, and absorption cross section is estimated to be  $\pm 10\%$ . More importantly, systematic errors in this absolute measurement can cause inaccurate results. Possible causes of systematic errors include the detection of light other than 185 nm, impurities in the gas flows, and interactions of the gases with surfaces. Several tests and measurements have been performed to ensure that the measurements are performed without intrinsic errors.

This UV absorption instrument has been tested by measuring the absorption cross section of an inert gas that can be easily sampled in large concentrations and comparing the results with published data. Nitrous oxide ( $\text{N}_2\text{O}$ ) has a well-known, large, and unstructured absorption section near 185 nm, and a cross section that decreases orders of magnitude at longer wavelengths (17). Hence, the detection of light at longer wavelengths (254 nm, for example) would result in an inaccurate determination of the absorption cross section. By diluting  $\text{N}_2\text{O}$  in a flow of  $\text{N}_2$  by approximately a factor of 100 (Figure 4), the absorption cross section of  $\text{N}_2\text{O}$  is measured at 297 K and 835 hPa to be  $1.40 \pm 0.04 \times 10^{-19} \text{ cm}^2$ , in agreement with the value of  $1.43 \pm 0.03 \times 10^{-19} \text{ cm}^2$  at 302 K reported by Selwyn et al. (17). Using  $\text{N}_2\text{O}$ , which does not readily react on surfaces, provides a convenient diagnostic of instrument performance and establishes that the absorption of 185 nm light is measured accurately.

The possibility that trace gases were lost on or through surfaces in the absorption cell apparatus was also examined. Although most components of the system are made from Teflon parts that rapidly passivate to  $\text{HNO}_3$  (15) or  $\text{NH}_3$  at the ppmv levels used here, reactions of  $\text{HNO}_3$  or  $\text{NH}_3$  on the fused silica windows at the ends of these cells could cause inaccurate measurements. The concentration and residence time of the gas-phase species within the cell were varied by changing the flow of the  $\text{N}_2$  carrier gas through the system and by changing the pressure in the cell. The concentration of  $\text{HNO}_3$  or  $\text{NH}_3$  in the absorption cell was varied by a factor of 5 by changing the flow of  $\text{N}_2$  carrier gas between 10 and 50 sccm. For example, the absorption caused by  $\text{NH}_3$  from a permeation tube varied from 0.6% to 1.4% by changing the flow from 50 sccm to 20 sccm, as shown in Figure 6. At lower flow rates, the concentration of the absorbing gas increases, such that the differential absorption increases. The emission rate derived using eq 3 was 102 ng/min for the three measurements shown in Figure 6 and was independent of flow and  $\text{NH}_3$  concentration in the absorption cell. The concentration was also varied by restricting the flow at the cell exit to increase the pressure in the cell up to 2500 hPa. Again, the derived emission rate was independent of pressure and trace gas concentration in the cell. Since large changes in the gas absorber number density and residence time in

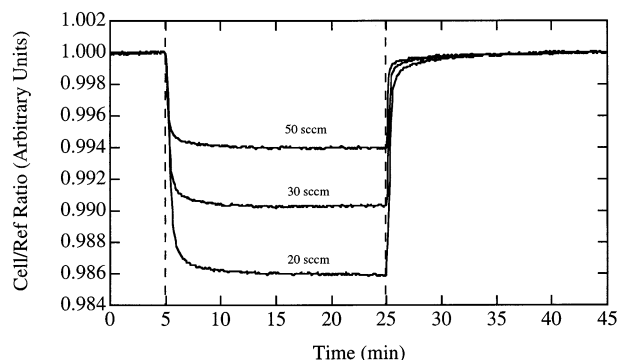


FIGURE 6. The absorption caused by a 102 ng/min  $\text{NH}_3$  permeation tube at different  $\text{N}_2$  carrier gas flows, as indicated on the figure. The vertical dashed lines indicate when the valve was actuated to admit and remove the  $\text{NH}_3$  from the absorption cell.

the absorption cell did not alter the derived permeation tube emission rates, wall effects that could cause systematic measurement errors are shown to be negligible at the ppmv-level mixing ratios used here.

The possibility that the measurement could be compromised by the presence of other absorbers in the system was assessed. If the carrier gas or any other components of the system upstream of the permeation tube oven contain  $\text{NH}_3$ ,  $\text{HNO}_3$ ,  $\text{O}_2$ , or any other molecule that absorbs at 185 nm, this differential measurement will not be affected. The gas always flows through all components of the system, including the scrubber and the oven. Consequently, absorbers that are removed by the scrubber will have no effect on the signals, and those that are not will reduce  $I$  and  $I_0$  by the same fraction, such that the ratio  $I/I_0$  is unchanged. If the Teflon components of the permeation tube oven, which is alternatively placed upstream and downstream of the scrubber to determine the differential absorption, release absorbers that are removed by the scrubbers, inaccurate measurements would result. Periodically, the permeation tube is removed from the oven, and the signals are examined to diagnose possible offsets in the measurement. The differential absorption quickly drops to zero, indicating that the measured absorption is a consequence of the permeation emission alone.

Although the measured permeation rates are independent of carrier gas flow and pressure, the permeation tube, oven, and absorption cell must equilibrate to changes in concentration of the trace gas within the system. Following changes in carrier gas flow between 20 and 50 sccm, both the  $\text{HNO}_3$  and  $\text{NH}_3$  permeation tubes equilibrated rapidly ( $<1/2$  h), as shown in Figure 7. When the carrier gas flow was changed, the change in absorption corresponded to the dilution of the trace gas, and the emission rate calculated using eq 3 remained constant. A permeation tube used to calibrate the inlet of an aircraft or balloon-based instrument might be exposed to pressure changes that approach 1 atm during rapid ascents or descents. When the pressure surrounding a permeation tube was changed from 835 hPa to approximately 1800 hPa (a pressure change of  $\sim 1$  atm), the permeation tube output returned to the original value in approximately 1 h (Figure 8). The importance of controlling the pressure surrounding a  $\text{HNO}_3$  permeation tube has been noted previously by Talbot et al. (2), and the results here show how the output from a calibration system can change in response to transients in pressure. The changes in permeation tube output observed here may be partially or entirely caused by the adsorption of  $\text{HNO}_3$  or  $\text{NH}_3$  on the Teflon oven and tubing. The results shown in Figure 8 are consistent with increased surface adsorption in response to the increase in concentration of the trace gas when the pressure was elevated, such that the output of the calibration

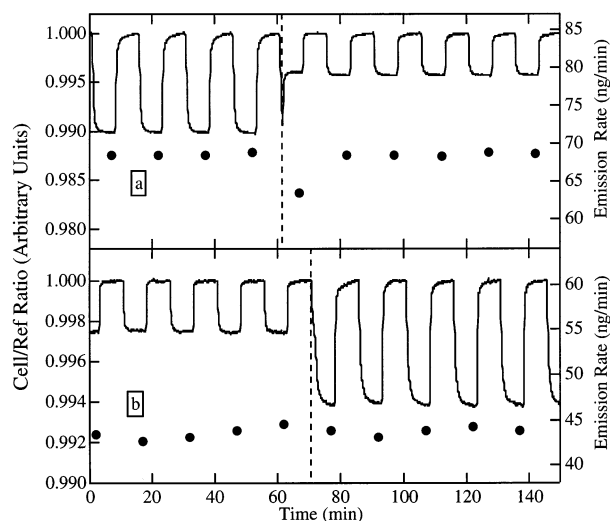


FIGURE 7. The solid lines (left axis) are the ratio of the cell detector signal to the reference detector signal, with the maximum value normalized to 1. The circles (right axis) are the derived permeation tube emission rates. A value is determined for each 30 min calibration cycle. The dashed vertical lines indicate when the flow of carrier gas through the system was changed. Panel a shows results for changing the  $\text{N}_2$  flow around a  $\text{HNO}_3$  permeation tube from 20 sccm to 50 sccm at 62 min. Panel b shows the results when the flow of  $\text{N}_2$  around a  $\text{NH}_3$  permeation tube is changed from 50 sccm to 20 sccm at 72 min.

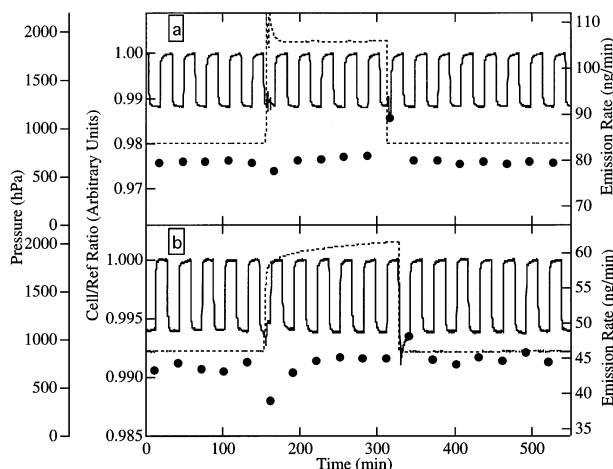


FIGURE 8. The solid lines (left axis) are the ratio of the cell detector signal to the reference detector signal, with the maximum value normalized to 1. The circles (right axis) are the derived permeation tube emission rates. A value is determined for each 30 min calibration cycle. The dashed lines (far left axis) are the pressures surrounding the permeation tubes. Panel a shows results for changing the pressure in a  $\text{HNO}_3$  permeation tube oven, and panel b shows the results for changing the pressure in a  $\text{NH}_3$  permeation tube oven.

system was initially reduced. Similarly, when the pressure surrounding the permeation tube was reduced, the wetted surfaces initially released the trace gas, and the output was elevated until the surfaces equilibrated to the new conditions. Since the difference in  $\text{NH}_3$  or  $\text{HNO}_3$  vapor pressure between the inside and outside of a permeation tube changed negligibly with these changes in pressure, the permeation devices equilibrated to the same emission rate. Calibration systems with larger surface areas would be expected to exhibit larger changes in output and longer equilibration times than shown in Figure 8. Consequently, it is recommended that the entire calibration system, including both the permeation tube oven and the tubing leading from the oven to the

instrument being calibrated, is pressure-controlled and the surface area is minimized.

The calibration of permeation tube emission rates by UV optical absorption has been compared to analysis by IC. The output from two HNO<sub>3</sub> permeation tubes was sent through a glass bubbler containing 20 mL of deionized water. For each measurement, the HNO<sub>3</sub> was bubbled between 1.5 and 4 h, to guarantee sufficient accumulation of nitrate for analysis by IC. Deionized water that had not been exposed to the output from the permeation tube was also analyzed, and the background nitrate was determined to be negligible. The IC analysis for the two different HNO<sub>3</sub> permeation tubes yielded 104 ± 4 ng/min and 31 ± 1 ng/min, where the uncertainties are determined from the standard deviation in the measurement of all the samples for each permeation tube. The UV absorption measurements of the same permeation tubes yielded 96 ng/min and 33 ng/min, where the uncertainty in each measurement is 10% as discussed above. Hence, the calibration of these permeation tubes by IC analysis and UV optical absorption are equivalent within the experimental uncertainties, and the system described here is demonstrated to accurately quantify the emission of HNO<sub>3</sub> and NH<sub>3</sub> from permeation tubes.

### Acknowledgments

We thank J. B. Burkholder for helpful discussions and R. B. Norton, A. Sullivan, and R. Weber for IC analysis of the permeation tubes.

### Literature Cited

- (1) Huey, L. G.; Dunlea E. J.; Lovejoy, E. R.; Hanson D. R.; Norton R. B.; Fehsenfeld F. C.; Howard, C. J. *J. Geophys. Res.* **1998**, *103*, 3355–3360.
- (2) Talbot, R. W.; Dibb, J. E.; Scheuer, E. M.; Blake, D. R.; Blake, N. J.; Gregory, G. L.; Sachse, G. W.; Bradshaw, J. D.; Sandholm, S. T.; Singh, H. B. *J. Geophys. Res.* **1999**, *104*, 5623–5634.

- (3) Neuman, J. A.; Huey, L. G.; Dissly, R. W.; Fehsenfeld, F. C.; Flocke, F.; Holecek, J. C.; Holloway, J. S.; Hubler, G.; Jakoubek, R.; Nicks, D. K.; Parrish, D. D.; Ryerson, T. B.; Sueper, D. T.; Weinheimer, A. J. *J. Geophys. Res.* **2002**, *107*, 4436, doi:10.1029/2001JD001437.
- (4) Maria, P.-C.; Gal, J.-F.; Balza, M.; Pere-Trepat, E.; Tumbiolo, S.; Couret, J.-M. *Anal. Chem.* **2002**, *74*, 305–307.
- (5) Mitchell, G. D.; Dorko, W. D.; Johnson, P. A. *Fresenius J. Anal. Chem.* **1992**, *344*, 229–233.
- (6) Fried, A. F.; Henry, B.; Sewell, S. *J. Geophys. Res.* **1998**, *103*, 18895–18906.
- (7) Proffitt, M. H.; Steinkamp, M. J.; Powell, J. A.; McLaughlin, R. J.; Mills, O. A.; Schmeltekopf, A. L.; Thompson, T. L.; Tuck, A. F.; Tyler, T.; Winkler, R. H.; Chan, K. R. *J. Geophys. Res.* **1989**, *94*, 16457–16555.
- (8) Huey, L. G.; Hanson, D. R.; Howard, C. J. *J. Phys. Chem.* **1995**, *99*, 5001–5008.
- (9) Wine, P. H.; Ravishankara, A. R.; Kreutter, N. M.; Shah, R. C.; Nicovich, J. M.; Thompson, R. L.; Wuebbles, D. J. *J. Geophys. Res.* **1981**, *86*, 1105–1112.
- (10) Biau, F. *J. Photochem.*, **2** **1973/74**, 139–149.
- (11) Burkholder, J. B.; Talukdar, R. K.; Ravishankara, A. R.; Solomon S. *J. Geophys. Res.* **1993**, *98*, 22937–22948.
- (12) Lovejoy, N. *Int. J. Mass Spectrom.* **1999**, *190/191*, 231–241.
- (13) Froyd, K. Ph.D. Thesis, University of Colorado at Boulder, 2002.
- (14) Tannenbaum, E.; Coffin, E. M.; Harrison, A. J. *J. Chem. Phys.* **1953**, *21*, 311–318.
- (15) Neuman, J. A.; Huey, L. G.; Ryerson, T. B.; Fahey, D. W. *Environ. Sci. Technol.* **1999**, *33*, 1133–1136.
- (16) *Handbook of Chemistry and Physics*, 66th ed.; Weast, R. C., Ed.; CRC Press: Boca Raton, FL, 1986.
- (17) Selwyn, G.; Podolske, J.; Johnston, H. S. *Geophys. Res. Lett.* **1977**, *4*, 427–430.

Received for review December 13, 2002. Revised manuscript received April 16, 2003. Accepted April 23, 2003.

ES026422L